



Removal of perfluorooctanoic acid from water with economical mesoporous melamine-formaldehyde resin microsphere



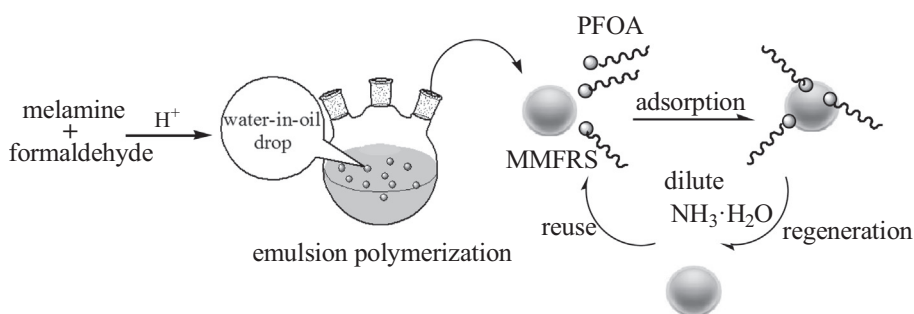
Jing Li, Qian Li, Lu-shuang Li, Li Xu*

Tongji School of Pharmacy, Huazhong University of Science and Technology, Wuhan 430030, China

HIGHLIGHTS

- Mesoporous melamine-formaldehyde resin microsphere was fabricated.
- It had high adsorption amount of perfluorooctanoic acid than activated carbon.
- The adsorption can be performed in a wide pH and temperature range.
- The material could be well regenerated by dilute ammonia solution.
- It was a potential adsorbent to remove perfluorooctanoic acid from water.

GRAPHICAL ABSTRACT



ARTICLE INFO

Article history:

Received 16 January 2017

Received in revised form 14 March 2017

Accepted 16 March 2017

Available online 18 March 2017

Keywords:

Melamine-formaldehyde
Microsphere
Perfluorooctanoic acid
Adsorption
Regeneration
Powdered activated carbon

ABSTRACT

Perfluoroalkyl and polyfluoroalkyl substances are priority contaminants of global concern. It is urgent to remove them from the environment. Adsorption is an efficient approach, but the adsorption capacity and regeneration of adsorbent were not satisfactory. In the present study, mesoporous melamine-formaldehyde resin microsphere (MMFRS) was fabricated through suspension polymerization. Owing to its mesoporous property and large anion-exchange capacity of 0.3 mmol/g, MMFRS was applied to the adsorption of perfluorooctanoic acid, a model target. The sorption kinetics obeyed pseudo-second-order equation and the sorption isotherms fitted both Freundlich and Langmuir models well. MMFRS exhibited a superiority over commercial powdered activated carbon on the adsorption amount. The sorption could reach equilibrium within 24 h. In addition, the material could be easily and economically regenerated by dilute $\text{NH}_3 \cdot \text{H}_2\text{O}$ (7.5 mM); a regeneration percentage (>85%) after 20 recycles was obtained. This study provides a facile, environmentally-friendly and low energy-consumption strategy for removal of perfluorooctanoic acid from aqueous solution in waste-water treatment.

© 2017 Elsevier B.V. All rights reserved.

1. Introduction

Perfluoroalkyl and polyfluoroalkyl substances (PFASs) are characteristic of C–F bond instead of C–H partially or completely in their structures. They are included in the Environmental Protection Agency's Contaminant Candidate List 3 of chemicals [1,2], which are related to low birth weight [3], thyroid disease [4], early

menopause for women [5], children's attention deficit or hyperactivity disorder [6] and even kidney and testicular cancer [7]. They are ubiquitous in the environment [8,9], as they are widely applied in manufacturing industry including non-stick cookware, firefighting foams, photographic films and coating materials for food packing, etc [2,8]. Since these compounds are extremely persistent and bioaccumulative in organism through the contaminated environment [2], removal of PFASs from environment has recently been of global concern. However, owing to the stable C–F bond in the structure, PFASs were resistant to most frequently-used water

* Corresponding author.

E-mail address: xulpharm@mails.tjmu.edu.cn (L. Xu).

treatment techniques, such as coagulation, filtration, aeration, oxidation and disinfection. Hence, some neoteric treatments were explored for this purpose, such as plasma-based method [10], electrocoagulation [11], electron beam treatment [12] and photocatalytic decomposition [13]; while these technologies were complicated and/or high-capital required. Hence, adsorption is still the most popular method to remove PFASs [14–19]. The activated carbon which possesses considerable large surface area is the most preferred adsorbent, for its high adsorption capacity and low cost, but seldom for regeneration. Thus, various reusable materials were explored, including, but not limited to, surface-modified silica [20,21], multi-walled carbon nanotubes [22] and molecularly imprinted polymers [14]. Although these adsorbents had some superiority in terms of regeneration, they hardly had comparable or higher adsorption capacity over the activated carbons; in addition, the synthesis processes were not facile and economical. Hence, an adsorbent which simultaneously possesses large adsorption capacity and easy regeneration property is highly desired for the PFASs treatment.

Porous polymer, especially resin microsphere, has gained heightened attention for their porous networks and large surface areas in diverse applications. Particularly, as the adsorbent, resin microsphere has the characteristics of high dispersibility in solvents, large surface area and applicability to multiple operational formats. Melamine-formaldehyde (MF) resin was well known for its rich imino groups and triazine rings, which endowed the material electropositivity in acid, neutral and weak basic environment. The MF resin microsphere was fabricated through various approaches, including dilute solution precipitation polymerization [23], sol-gel method [24], hydrothermal method [25], template synthesis method [26] and dispersed polycondensation [27], etc. They found some applications as adsorbents for ionic dyes [28], CO₂ [29] and heavy metal ions [30]. Herein, taking advantages of both resin microsphere and MF resin, mesoporous melamine-formaldehyde resin microsphere (MMFRS) was deliberately fabricated through suspension polymerization. MMFRS was then applied to adsorb perfluorooctanoic acid (PFOA), one of the representative of PFASs. The regeneration ability of MMFRS was especially tested. The study would provide an alternative strategy to remove PFASs from the environment.

2. Experimental

2.1. Materials

Melamine, formaldehyde (37%, wt%), polyethylene glycol 20000 (PEG 20000), petrol ether (60 °C–90 °C), ammonium hydroxide (NH₃·H₂O), ethanol (EtOH), phenol, CH₂Cl₂, NH₄AcO, HCl, NaOH, NaCl, KCl, CaCl₂, MgSO₄, CuSO₄, sodium dodecyl sulfonate (SDS), humic acid, Triton X-100 and lauryl dimethyl amine oxide (OB-2) of analytical reagent grade and powdered activated carbon (PAC, 5–10 μm) were all obtained from Sinopharm Chemical Reagent Co., Ltd. (Shanghai, China). PFOA (90%) and estradiol were purchased from Aladdin Chemical Reagent Co., Ltd. (Shanghai, China). High performance liquid chromatography (HPLC)-grade acetonitrile (ACN) was bought from Sigma-Aldrich Trading Co., Ltd. (Shanghai, China). Deionized water was produced with a Heal Fore NW system (Shanghai, China).

2.2. Preparation and characterization of MMFRS

MMFRS was fabricated by suspension polymerization, which is one of the popular heterogeneous polymerization method for the preparation of monodispersed polymer spheres. The detailed scheme was as follows. Melamine (12.5 g) and PEG 20,000 (6.0 g)

were dissolved in formaldehyde solution (37%, 80 mL) at 50 °C under stirring till the solution became transparent, followed by filtration through polypropylene membrane to remove the insoluble particles, and the filtrate was the MF prepolymer solution. After the prepolymer solution was cooled down to room temperature, HCl solution (0.84 M, 4 mL) as a catalyst was added. Then, the oil phase, i.e. petrol ether (196 mL) containing Triton X-100 (1.4 g) and OB-2 (1.4 g), was poured into the prepolymer solution. With the agitation at 500 rpm and 50 °C, the water phase (the prepolymer solution) was mixed well with the oil phase for reaction. After 10 h, white suspension was formed, and the solid was collected by filtration and washed with petrol ether, ethanol and deionized water successively; thus-obtained material was MMFRS. To enhance the high three-dimensional cross-linking degree and thermostability, the material was hydrothermally treated at 140 °C for 10 h in a polytetrafluoroethylene pressure vessel. Afterwards, the material was centrifuged, dried at 80 °C and stored in a desiccator before use.

The obtained material was characterized as below. A JSM-35CF scanning electron microscopy (SEM) (JEOL, Japan) and a JEM-2100 HR transmission electron microscope (TEM) (JEOL, Japan) were used for morphology and porosity observation. An AVATAR 360 transform infrared spectrometer (FT-IR) (Thermo, USA) was used to characterize the functional groups. To analyze the thermal behavior of the material, thermogravimetric analysis (TGA) and differential scanning calorimetry (DSC) were conducted on a TG 209 F1 Libra thermogravimetric analyzer (NETZSCH, Germany) and a Q2000 DSC differential scanning calorimeter (TA instruments, USA), respectively. The nitrogen adsorption isotherms for porous characterization were obtained on a TriStar II surface area analyzer (Micromeritics, USA). The zeta potential of MMFRS was measured by a ZetaPALS Zeta Potential Analyzer (Brookhaven, USA).

The anion-exchange capacity of MMFRS was determined by conductometric titration with a DDS-307 conductivity meter (Leici, Shanghai, China), referred as previous literature [31]. Typically, MMFRS (50 mg) was dispersed in 5 mL NaOH (0.1 M), and titrated by HCl (20 mM). Accordingly, the conductivity of the system was recorded to calculate the anion-exchange capacity of MMFRS (mmol/g resin). The pK_a value of MMFRS was determined by the potentiometric titration method with a Delta 320 pH meter (Mettler Toledo, Shanghai, China).

2.3. Batch adsorption experiments

The general adsorption experiment was carried out as below. MMFRS (10 mg) was added to the PFOA aqueous solution (700 ppm, 4 mL), adjusted with HCl or NaOH to the desired pH. The adsorption was assisted by a SPX-250B-D constant shaking incubator (Boxun, Shanghai, China) at 50 rpm and 25 °C for 24 h. After adsorption, the solution was filtrated and the filtrate was injected to a HPLC-evaporative light scattering detector (HPLC-ELSD) system to determine the residual concentration of PFOA. The HPLC-ELSD system consisted of a Shimadzu (Tokyo, Japan) LC-20AD pump, a Dionex C18 column (4.6 × 150 mm, 5 μm, USA), and an Alltech 2000ES ELSD (Grace, USA). The mobile phase was 55% NH₄AcO (20 mM)–45% ACN at a flow rate of 0.5 mL/min and a column oven of 40 °C. The temperature of drift tube was 100 °C, and the flow rate of carrier gas (N₂), which was produced from a WSK-A auto air generator (Tianjin, China), was set at 2.8 mL/min.

The effects of sample pH, temperature and the coexisting pollutants on the adsorption and adsorption process were studied. (1) To investigate the effect of pH on adsorption, the pH of PFOA solution (700 ppm) was adjusted with HCl or NaOH to the desired pH as specified and the adsorption was conducted at room temperature. The following experiments were conducted without pH adjust-

ment. (2) To investigate the effect of temperature, the temperature ranged from 15 °C to 50 °C, and the PFOA concentration was 700 ppm. The subsequent experiments were conducted at room temperature. (3) In the effects of inorganic salts and organic pollutants, PFOA (700 ppm) spiked with individual substance of specified concentration was applied. (4) In the adsorption isotherm experiments, the initial concentration of PFOA ranged from 500 ppm to 1500 ppm; while for adsorption kinetics experiments, 1500 ppm of PFOA was adopted. The concentration of PFOA in the solution at equilibrium or specified time point was determined. All the experiments were carried out in triplicate. The adsorption amount was calculated by the difference between the concentrations of PFOA solution before and after adsorption. Adsorption percentage (%) was the ratio of the adsorption amount to the initial amount. For comparison, PAC instead of MMFRS was used.

2.4. Regeneration and reusability

After adsorption, the PFOA-adsorbed materials were separated and immersed in $\text{NH}_3\cdot\text{H}_2\text{O}$ (7.5 mM, 3.5 mL) for 20 min, washed with deionized water till neutral, and then dried at 80 °C for the next adsorption cycle. The regeneration conditions, including solvent, desorption mode, desorption times and concentration of $\text{NH}_3\cdot\text{H}_2\text{O}$, were all optimized in detail. In the case of PAC, both EtOH and $\text{NH}_3\cdot\text{H}_2\text{O}$ were used as the regeneration solvent for comparison.

3. Results and discussion

3.1. Synthesis of MMFRS

The synthesis of MMFRS via suspension polymerization was depicted in Fig. 1. (I) In the prepolymer solution, hydroxymethyl groups were formed by the nucleophilic attack of formaldehyde

to the hydrogen atom of the $-\text{NH}_2$ in the triazine ring of melamine molecules [32]; (II) When the prepolymer solution was dispersed into the oil phase under mechanical agitation, water-in-oil drop was formed; (III) The melamine molecules were cross-linked through the formation of methylene or methylene ether bridges [33,34] with the rising reaction temperature (50 °C) in the presence of the catalyst (HCl); (IV) The branched polymer species formed into small clusters which could act as the nucleation sites; (V) The small clusters with plenty of unreacted sites could continuously grow and aggregate to form microspherical particles finally. With the subsequent hydrothermal treatment, the degree of three-dimensional crosslink and thermostability were enhanced.

3.2. Characterization of MMFRS

As shown in Fig. 2(a), the particle size of MMFRS was approximately 5–15 μm . From the TEM image in Fig. 2(b), the average pore size of the mesopores was estimated to be ca. 10 nm, which agreed well with the result (~ 11 nm) obtained by nitrogen adsorption-desorption isotherms as shown in Fig. 3(a); while, the average pore size of PAC was calculated to be around 3.5 nm based on the Barrett-Joyner-Halenda method (Fig. 3(b)). The specific surface area of MMFRS was determined and calculated to be 291 m^2/g based on the Brunauer-Emmett-Teller model, which is much lower than that of PAC (1539 m^2/g). Whereas, from the nitrogen adsorption-desorption isotherms in Fig. 3(b), it could be seen that, unlike MMFRS, large amount of micropores existed in PAC.

Fig. 4 depicts FT-IR spectra of MMFRS. The broad band at 3421 cm^{-1} was attributed to the amino groups ($-\text{NH}_2$) and possible residual trace H_2O though all the samples were dried under vacuum at 80 °C. The medium peak appeared at 2951 cm^{-1} may be assigned to the stretching vibration of imino groups ($-\text{NH}-$). The obvious signals at 1550 and 811 cm^{-1} were typical of 1,3,5-triazine ring. The weak peaks at 1490 and 1190 cm^{-1} should be

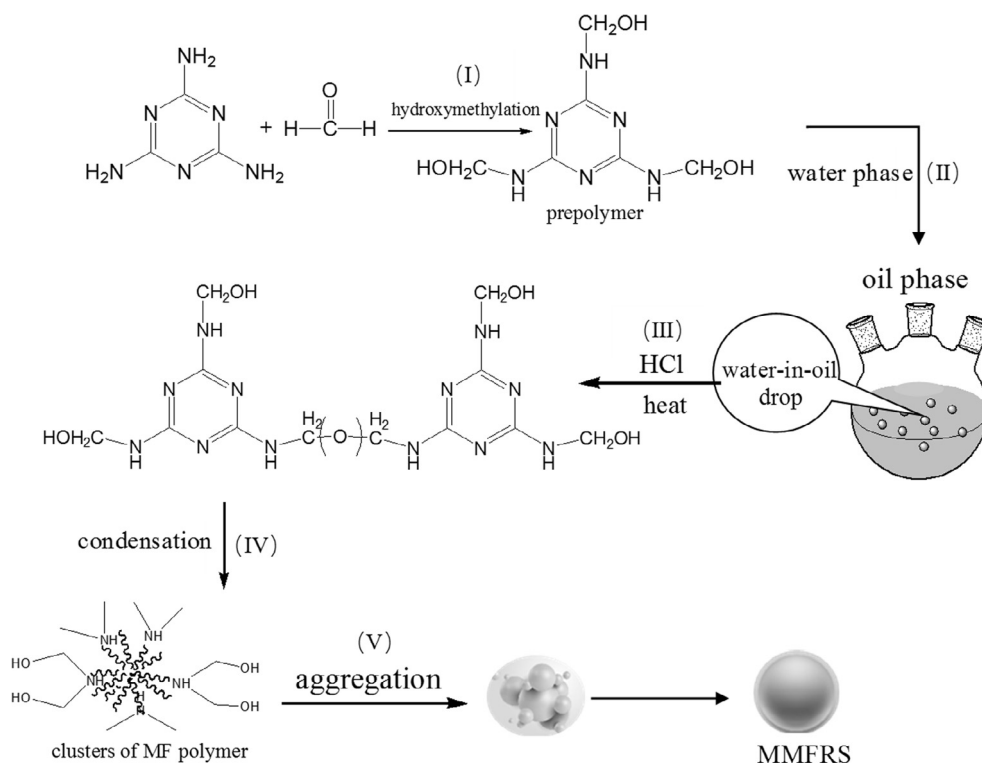


Fig. 1. Schematic illustration of the synthesis of MMFRS.

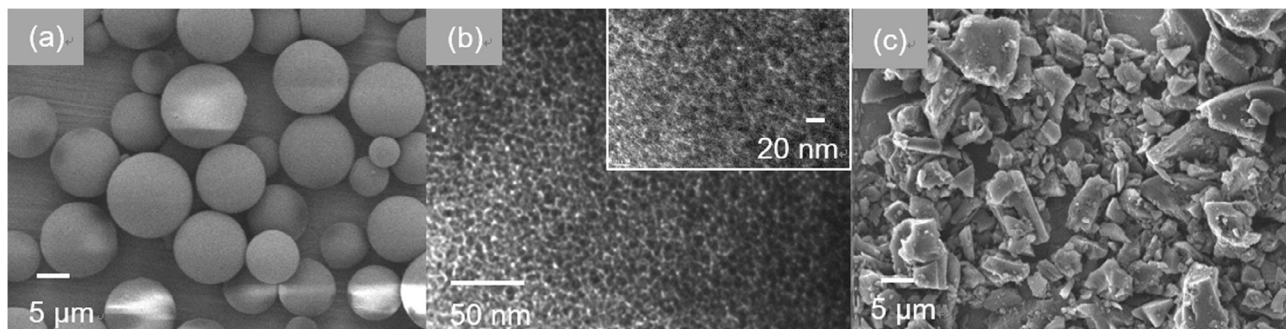


Fig. 2. SEM and TEM characterization of the adsorbents: (a) SEM image of MMFRS (b) TEM image of MMFRS; (c) SEM image of PAC.

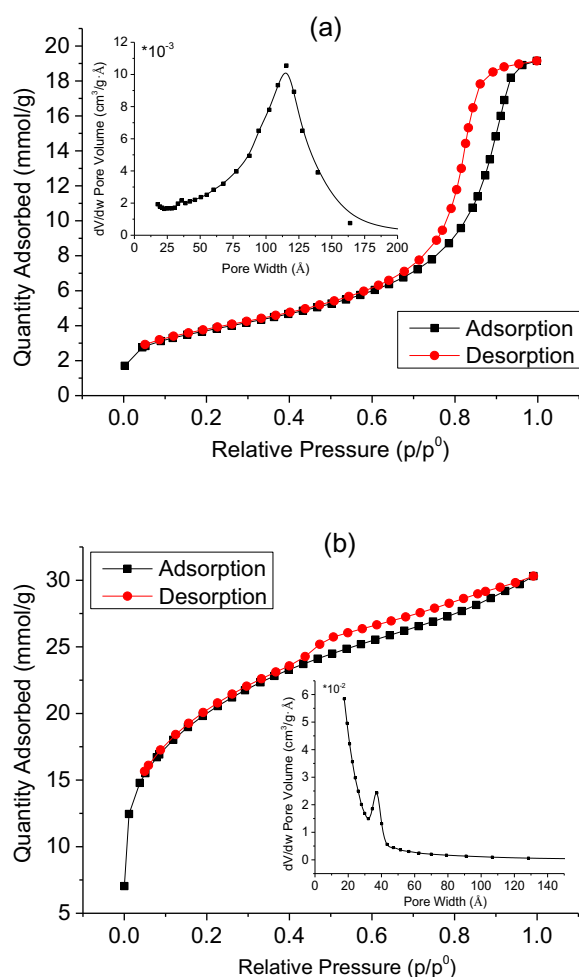


Fig. 3. Nitrogen adsorption-desorption isotherms and mesopore size distributions of (a) MMFRS and (b) PAC.

resulted from methylene; the weak peak at 986 cm^{-1} belonged to the hydroxymethyl groups. The FT-IR spectrum of the prepared MMFRS agreed well with previously reported MF materials [23].

Fig. 5 exhibits the TGA (a) and DSC (b) curves of MMFRS. As seen in Fig. 5(a), tremendous mass lost occurred between 400 °C and 800 °C ; when the temperature rose to 800 °C , MMFRS was completely decomposed, which was in accordance with Ming's report [23]. The tiny mass change before 200 °C might be attributed to the loss of water and the dehydration of hydroxyls in the molecule. In addition, no thermal degradation peak was observed on the DSC curve in Fig. 5(b) from room temperature to 200 °C , which demonstrated that MMFRS was stable up to 200 °C .

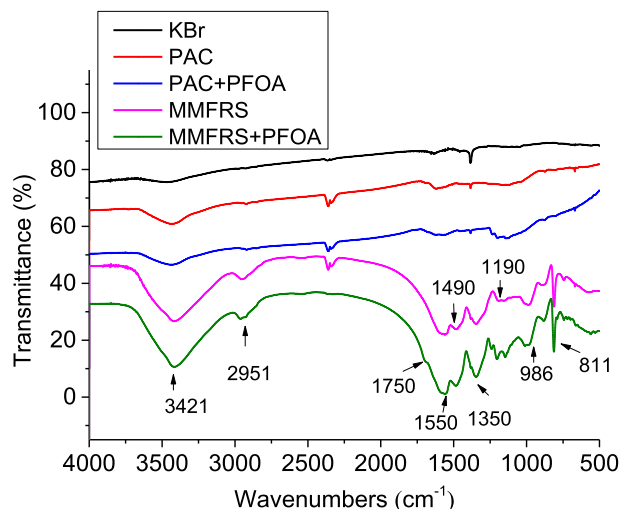


Fig. 4. FT-IR spectra of the adsorbents before and after adsorption of PFOA.

Fig. 6(a) depicts the conductometric titration curve. When HCl was dripped into the MMFRS/NaOH system, NaOH would be firstly neutralized, which resulted in the sharp change of ion concentration in system, reflected by the changing conductivity of the solution. After all the OH^- of NaOH was reacted, $-\text{NH}-$ of MMFRS would be deprotonated and participate in the neutralization reaction with HCl, contributing to a platform in the conductometric titration curve. On basis of the volume of HCl consumed in the platform, the anion-exchange capacity was calculated to be 0.3 mmol/g which was similar to the previous report [35].

Fig. 6(b) displays the potentiometric titration curve of MMFRS/NaOH. The pK_b value of MMFRS was calculated to be 8.13 [36]. In addition, zeta potential in deionized water was measured as $45.46 \pm 1.91\text{ mV}$. The results imply that, MMFRS is electropositive at the pH range of 2–10 for being protonated partially or entirely, and neutral in stronger basic environment.

From the above characterizations, MMFRS was successfully synthesized with acceptable specific surface area, suitable pore diameter and appreciable anion-exchange capacity in a wide pH range.

3.3. Parameters on adsorption

As shown in Fig. 4, after adsorption, the peaks at $1200\text{--}1300\text{ cm}^{-1}$ were split and strengthened owing to the stretching vibration of C-F, which could be observed in both MMFRS and PAC; the very weak peak at 1750 cm^{-1} was attributed to the carbonyl groups of PFOA. The results demonstrated that PFOA was adsorbed onto the material and the interaction between the

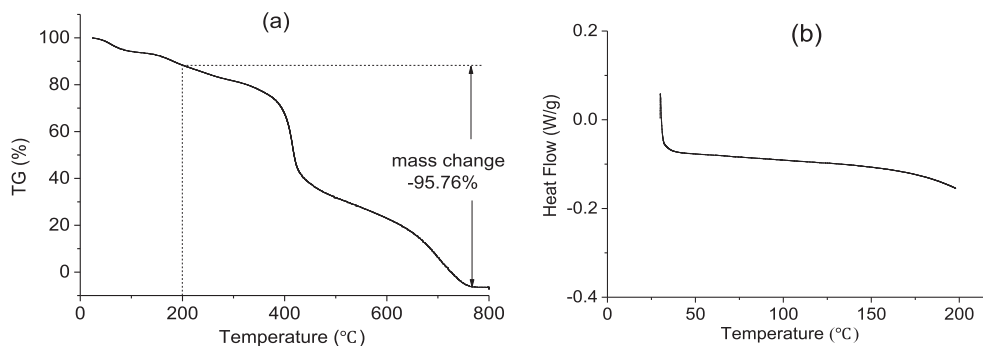


Fig. 5. TGA (a) and DSC (b) curves of MMFRS.

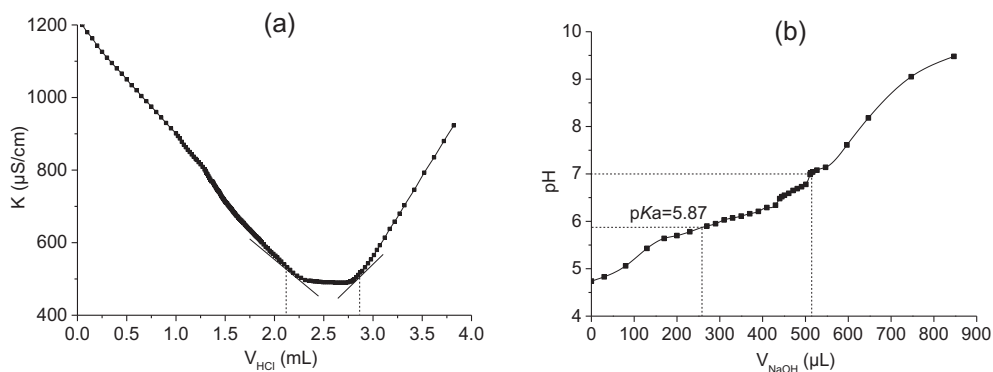


Fig. 6. Conductance (a) and potentiometric (b) titration curves of MMFRS. (K: conductivity of the HCl-NaOH/MMFRS titration reaction system).

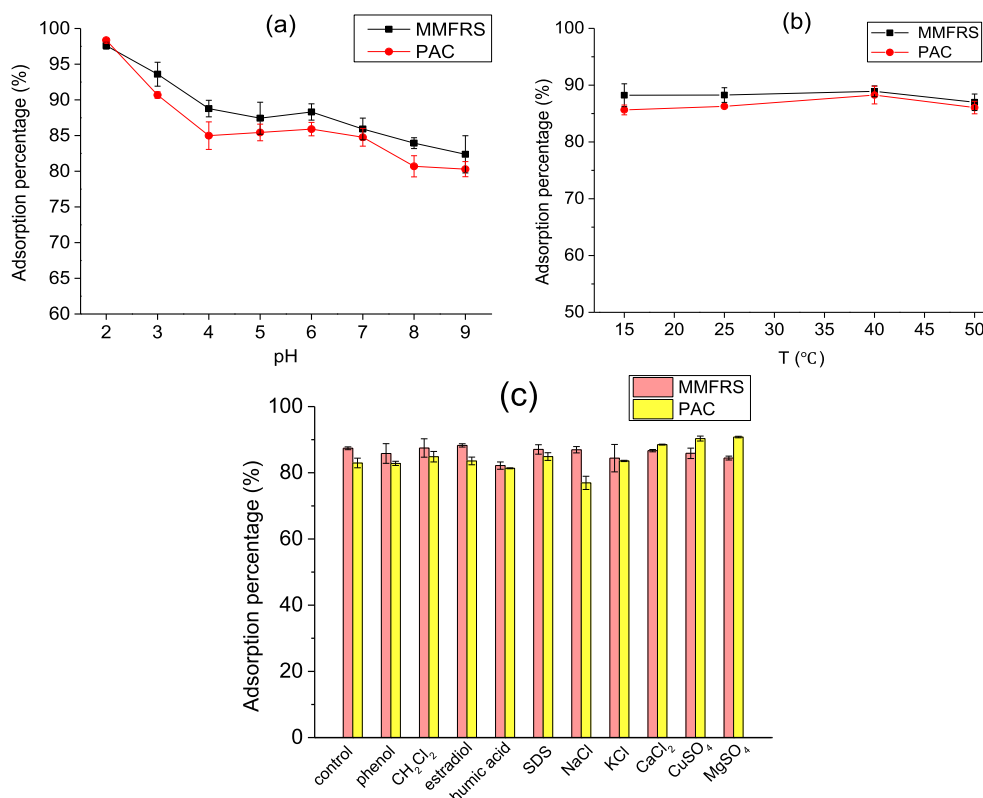


Fig. 7. Effect of pH (a), temperature (b) and interfering substances (c) on adsorption percentage (%) for PFOA. (Concentration of spiked NaCl, KCl, CaCl_2 , CuSO_4 and MgSO_4 : 5 mM; phenol, dichloromethane and estradiol: 1 $\mu\text{g}/\text{mL}$; SDS: 5 $\mu\text{g}/\text{mL}$; humic acid: 0.5 mg/mL).

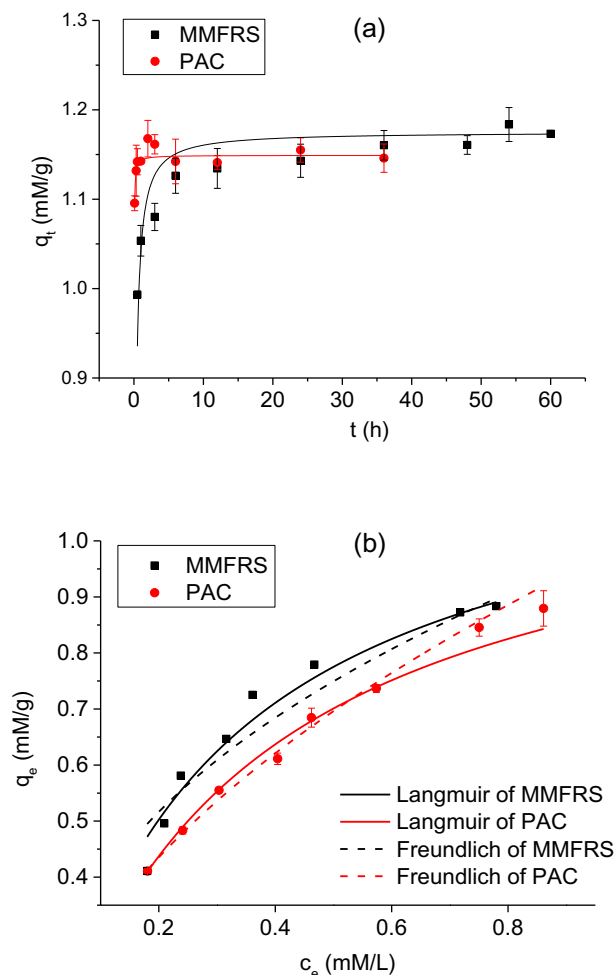


Fig. 8. Sorption kinetics (a) and isotherms (b) of MMFRS and PAC for PFOA. (q_t , amounts of PFOA versus time; q_e , amounts of PFOA adsorbed on adsorbent at equilibrium; c_e , the equilibrium concentration of PFOA in aqueous solution).

amino/imino groups and carboxyl groups in PFOA contributed to the adsorption.

The pH of sample solution and temperature could have influential effects on adsorption [14,37]. Fig. 7(a) displays the variation trend of adsorption percentage with the varied sample pH. As the pH of PFOA solution increased, the adsorption percentage decreased, which was consistent with the previous results [37–39]. It could be explained as follows. As PFOA has a pK_a of 2.8 [40], PFOA is partially deionized into PFO^- at pH 2–4.8 and ionized completely at higher pH range; while, with a pK_b of 8.13 as determined *vide supra*, MMFRS was electropositive at pH 2–10 for being protonated partially or entirely. At the pH of 2, ionic hydrogen bond interactions between carbonyl groups in PFO^- and $-NH_2^+$ in the protonated MMFRS dominated the adsorption; while, owing to the structural cavity in MMFRS, hydrophobic interaction could not be ignored; in addition, Cl^- (from HCl) in the ion pairs $NH_2^+-Cl^-$ could be exchanged by ionized PFO^- and electrostatic interaction might exist. When pH rose to 4, the ionization of PFOA was enhanced, which increased the relative proportion of PFO^- . Thus, the ionic hydrogen bond and anionic exchange interactions were slightly facilitated, while the hydrophobic interaction was weakened, which resulted in a reduction of adsorption percentage as a whole. With the increasing pH to 6, PFOA was almost deionized. The weakened hydrophobic interaction was counteracted by enhanced anionic exchange and ionic hydrogen bond interactions, thus producing a relatively stable adsorption percentage. When pH reached to 7–9, the protonation of MMFRS began to decline. The

anion exchange between the ion pair $NH_2^+-OH^-$ (OH^- originated from H_2O or NaOH.) and PFO^- , the ionic hydrogen and hydrophobic interactions were all weakened. Hence, the adsorption percentage continued to decrease.

Fig. 7(b) shows the influence of temperature on adsorption. With the increasing temperature from 15 °C to 40 °C, the adsorption percentage slightly increased correspondently, which may be due to the beneficial effect of higher temperature on mass transfer. However, with further increasing temperature to 50 °C, the adsorption percentage decreased, which could be resulted from increasing solubility of PFOA in water [39,41]. Anyway, the variation of adsorption percentage was not that significant with the temperature change.

The influence of coexisting inorganic and organic pollutants on the adsorption was conducted referring to previous reports [14,15,38]. In addition to common inorganic salts including NaCl, KCl, $CaCl_2$, $MgSO_4$ and $CuSO_4$, several representatives of organic pollutants including SDS, phenol, dichloromethane, estradiol and humic acid were also included. As shown in Fig. 7(c), in the presence of pollutants with not lower concentration than the normally reported residual concentration in the environment [42–47], the adsorption percentage was not significantly influenced. The result was analogous to Du's work [15].

From the above analysis, the temperature and interfering substances had slight influence on adsorption in both cases of MMFRS and PAC. In the pH range of 4–9 close to natural aquatic environment [37], the PFOA adsorption capacity only had small fluctuation, which means both MMFRS and PAC can be used for adsorption of PFOA in a wide pH and temperature range. In addition, under the same condition, MMFRS exhibited slight superiority over PAC in terms of adsorption capacity. Considering the facility for operation, all the subsequent experiments were conducted at room temperature (~ 25 °C) without pH regulation.

3.4. Sorption kinetics

The pores and the functional groups of the adsorbent could have a synergetic effect on the adsorption amount and rate [20]. The content of functional groups determined the quantity of the available active adsorption sites, and thus the interactions between PFOA and MMFRS, resulting in the different adsorption amounts and rates. The pores of the adsorbent not only guaranteed the considerable surface area, but also provided access for the analyte into the interior surface, which was also important for the adsorption amount and the mass transfer during adsorption.

To better know the adsorption behavior of MMFRS, herein, the sorption kinetics was studied, as shown in Fig. 8(a). MMFRS and PAC had a comparable equilibrium time, reaching equilibrium within 24 h. It can be explained that the average pore diameters of PAC and MMFRS were 11 nm and 3.5 nm, respectively, which were capacious for the mass transfer of PFOA with a molecule length of 1.2 nm [17]. Compared to other commercial ion-exchange resins [16], MMFRS possessed relatively larger mesopores, possibly resulting in rapid adsorption equilibrium of PFOA.

Table 1

Kinetic parameters of pseudo-second-order equation^a for PFOA adsorption on MMFRS and PAC.

| Adsorbents | Parameters | | |
|------------|------------|-------|--------|
| | q_e | v_0 | r^2 |
| MMFRS | 1.18 | 9.1 | 0.8152 |
| PAC | 1.15 | 214.2 | 0.8684 |

^a Pseudo-second-order equation: $q_t = \frac{q_e v_0}{q_e + v_0 t}$, where q_e is the amounts of PFOA adsorbed on adsorbent (mM/g) at equilibrium; v_0 is the initial sorption rate ($mM g^{-1} h^{-1}$).

Table 2
Fitting parameters of Langmuir and Freundlich equations for PFOA sorption onto MMFRS and PAC.

| Adsorbents | Langmuir ^a model | | | Freundlich ^b model | | |
|------------|-----------------------------|------|----------------|-------------------------------|------|----------------|
| | q _m | b | r ² | q _m | b | r ² |
| MMFRS | 1.21 | 3.53 | 0.9862 | 0.99 | 2.46 | 0.9678 |
| PAC | 1.17 | 2.98 | 0.9958 | 0.98 | 1.95 | 0.9926 |

^a Langmuir equation $q_e = \frac{b q_m c_e}{1 + b c_e}$,
^b Freundlich equation $q_e = k \cdot c_e^n$, where c_e is the equilibrium concentration of PFOA in aqueous solution (mmol L⁻¹g⁻¹); q_e is the equilibrium adsorption amount (mmol/g); q_m is the maximum sorption capacity (mmol/g) and n is an indication of the nonlinearity.

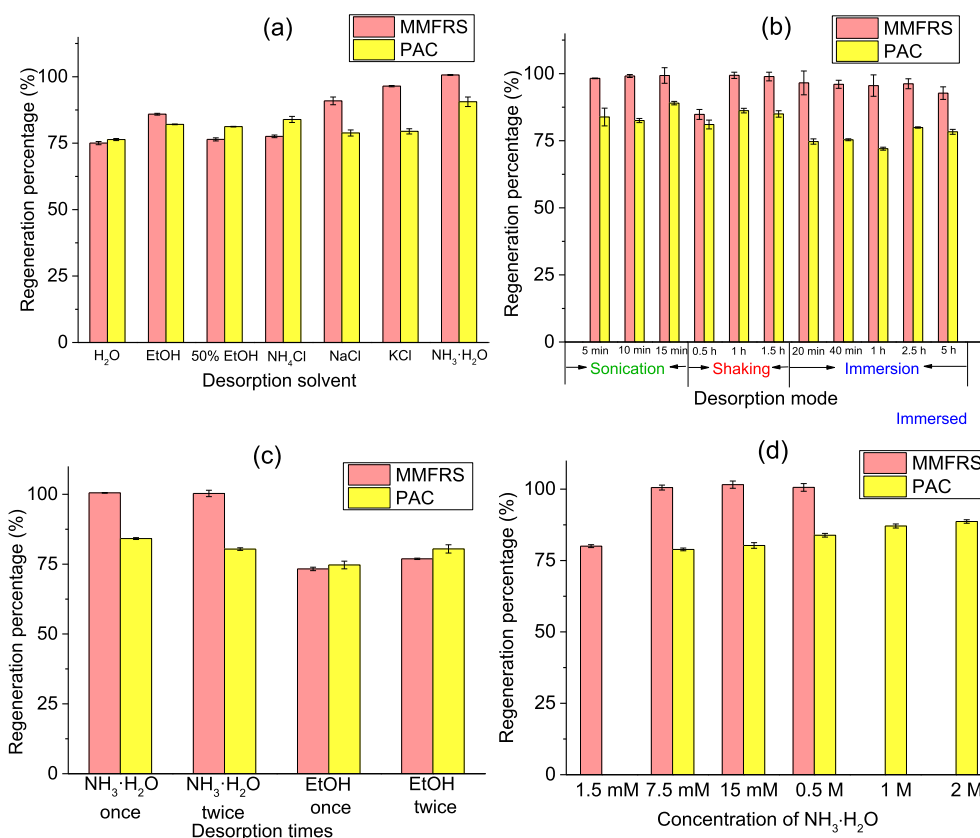


Fig. 9. Optimization of the desorption conditions for regeneration (a) solvent type; (b) desorption mode; (c) desorption times; (d) concentration of NH₃·H₂O.

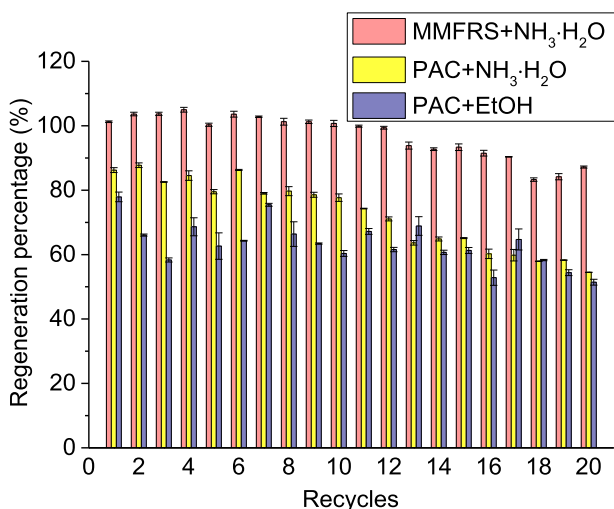


Fig. 10. Reusability of MMFRS and PAC in manifold adsorption recycles.

Pseudo-second-order equation was adopted to fit the sorption kinetic data. The detailed parameters are listed in Table 1. As shown in Fig. 8(a) and Table 1, the acceptable correlation coefficients (r^2) indicated that the adsorption of PFOA on the adsorbents conformed to the assumption that the adsorption rate was controlled by chemical sorption [48], and the results were consistent with most relevant reports [15,19,20].

3.5. Sorption isotherms

The sorption isotherms were obtained from the adsorption amount at different initial PFOA concentrations. Freundlich and Langmuir equations are most frequently-used models to simulate the sorption isotherms. Therefore, both of them were applied herein and the results are displayed in Fig. 8(b) and Table 2. It could be observed that all the isotherms exhibit nonlinear characters and the two models both fitted well with favorable r^2 . A good fitting for Langmuir equation indicates monolayer adsorption on the adsorbents, which further demonstrates that the chemical sorption was predominant [39]; whereas, the suitability of Freundlich equation means that the adsorption site was heterogeneous and multiple interactions existed in the adsorption [14,39].

The results were related to the stereochemical structure of MMFRS. The widespread imino groups and abundant cavities rendered MMFRS multiple sites to interact with PFOA in diverse ways.

3.6. Regeneration and reusability

Regeneration and reusability of the adsorbents are highly appreciated in industry for the consideration of economy, environmental friendliness and operational convenience. However, regeneration was not involved in some reports for the difficulty and inconvenience of the procedure. Punyapalukul [20] found that the reused PAC had a significant loss of adsorption capacity, while the functionalized silicas with better regeneration ability required a high synthesis cost. Yu's group [39] obtained a satisfactory regeneration percentage of 95% for the MIP adsorbents, while the mixture of acetone and NaOH as the regeneration solvent was not "green".

Herein, regeneration of MMFRS and PAC was attempted in parallel with different kinds of regeneration solvents, as shown in Fig. 9(a). Regeneration percentage was the ratio of the adsorption amount after the second operation to that of the first one. From Fig. 9(a), $\text{NH}_3\cdot\text{H}_2\text{O}$ had the best regeneration ability for both of the two adsorbents; while EtOH is nontoxic and feasible for recycle use in industry. Hence, both $\text{NH}_3\cdot\text{H}_2\text{O}$ and EtOH were selected for subsequent experiments. The desorption mode (including sonication, shaking and immersion), the repeated desorption times, as well as the concentration of $\text{NH}_3\cdot\text{H}_2\text{O}$ were studied in detail, and results are displayed in Fig. 9(b–d).

According to the above optimizations and considering the convenience of operation, adsorbents containing PFOA can be regenerated by being immersed in 7.5 mM $\text{NH}_3\cdot\text{H}_2\text{O}$ once for 20 min, then washed with water till neutral, and dried at 80 °C for reuse. The drying procedure was just for lab experiment to obtain more accurate data, which could be omitted in practical industry for convenience. The optimal condition was applied to the multiple cycles for the adsorbents and data is shown in Fig. 10. It could be observed encouragingly that MMFRS remained a regeneration percentage (>85%) after 20 recycles; while, unexpectedly, PAC possessed an acceptable reusability (about 50%) with $\text{NH}_3\cdot\text{H}_2\text{O}$, which is inconsistent with some reports [17,20]. Anyway, MMFRS possessed obviously superior reusability to PAC. To be specific, the regeneration of MMFRS and PAC with EtOH was also conducted. However, after 2 cycles, MMFRS became hydrophobic in the case of MMFRS as the adsorbent, possibly owing to incomplete desorption of PFOA from the adsorbent by EtOH, which lead to the difficulty for subsequent operations. Thus, EtOH was not suitable for the regeneration of MMFRS.

4. Conclusions

Mesoporous melamine-formaldehyde resin microsphere (MMFRS) was fabricated through suspension polymerization with high anion-exchange capacity. MMFRS can be used for adsorption of perfluorooctanoic acid in a wide pH and temperature range with the operational convenience. The sorption kinetics obeyed pseudo-second-order model and the sorption isotherms fitted both Freundlich and Langmuir models. MMFRS exhibited a superiority over powdered activated carbons in terms of the adsorption amount. Moreover, the sorption could reach equilibrium within 24 h, which may enhance the efficiency of treatment of wastewater. In addition, the MMFRS could be easily and economically regenerated by dilute $\text{NH}_3\cdot\text{H}_2\text{O}$, and possess favorable reusability (>85%) after manifold cycles. To sum up, MMFRS can be a potential and alternative adsorbent in practical industry for wastewater treatment.

Acknowledgements

The authors gratefully acknowledge the financial support of this research by the Program for New Century Excellent Talents in University (No. NCET-12-0213), Ministry of Education of China.

References

- [1] www.federalregister.gov/documents/2009/10/08/E9-24287/drinking-water-contaminant-candidate-list-3-final.
- [2] T.D. Appleman, C.P. Higgins, O. Quiñones, B.J. Vanderford, C. Kolstad, J.C. Zeigler-Holady, E.R. Dickenson, Treatment of poly- and perfluoroalkyl substances in U.S. full-scale water treatment systems, *Water Res.* 51 (2014) 246–255.
- [3] C. Fei, J.K. McLaughlin, R.E. Tarone, J. Olsen, Perfluorinated chemicals and fetal growth: a study within the Danish National Birth Cohort, *Environ. Health Persp.* 115 (2007) 1677–1682.
- [4] D. Melzer, N. Rice, M.H. Depledge, W.E. Henley, T.S. Galloway, Association between serum perfluorooctanoic acid (PFOA) and thyroid disease in the U.S. National Health and Nutrition Examination Survey, *Environ. Health Persp.* 118 (2010) 686–692.
- [5] S.S. Knox, T. Jackson, B. Javins, S.J. Frisbee, A. Shankar, A.M. Ducatman, Implications of early menopause in women exposed to perfluorocarbons, *J. Clin. Endocr. Metab.* 96 (2011) 1747–1753.
- [6] K. Hoffman, T.F. Webster, M.G. Weisskopf, J. Weinberg, V.M. Vieira, Exposure to polyfluoroalkyl chemicals and attention deficit/hyperactivity disorder in U.S. children 12–15 years of age, *Environ. Health Persp.* 118 (2010) 1762–1767.
- [7] V.M. Vieira, K. Hoffman, H.M. Shin, J.M. Weinberg, T.F. Webster, T. Fletcher, Perfluorooctanoic acid exposure and cancer outcomes in a contaminated community: a geographic analysis, *Environ. Health Persp.* 121 (2013) 318–323.
- [8] M.F. Rahman, S. Peldszus, W.B. Anderson, Behaviour and fate of perfluoroalkyl and polyfluoroalkyl substances (PFASs) in drinking water treatment: a review, *Water Res.* 50 (2014) 318–340.
- [9] F. Xiao, M.F. Simcik, T.R. Halbach, J.S. Gulliver, Perfluorooctane sulfonate (PFOS) and perfluorooctanoate (PFOA) in soils and groundwater of a U.S. metropolitan area: migration and implications for human exposure, *Water Res.* 72 (2015) 64–74.
- [10] G.R. Stratton, F. Dai, C.L. Bellona, T.M. Holsen, E.R.V. Dickenson, S.M. Thagard, Plasma-based water treatment: efficient transformation of perfluoroalkyl substances in prepared solutions and contaminated groundwater, *Environ. Sci. Technol.* 51 (2017) 1643–1648.
- [11] B. Yang, Y. Han, G. Yu, Q. Zhuo, S. Deng, J. Wu, P. Zhang, Efficient removal of perfluoroalkyl acids (PFAAs) from aqueous solution by electrocoagulation using iron electrode, *Chem. Eng. J.* 303 (2016) 384–390.
- [12] L. Wang, B. Batchelor, S.D. Pillai, V.S.V. Botlaguduru, Electron beam treatment for potable water reuse: removal of bromate and perfluorooctanoic acid, *Chem. Eng. J.* 302 (2016) 58–68.
- [13] M. Li, Z. Yu, Q. Liu, L. Sun, W. Huang, Photocatalytic decomposition of perfluorooctanoic acid by noble metallic nanoparticles modified TiO_2 , *Chem. Eng. J.* 286 (2016) 232–238.
- [14] Z. Du, S. Deng, Y. Bei, Q. Huang, B. Wang, J. Huang, G. Yu, Adsorption behavior and mechanism of perfluorinated compounds on various adsorbents—a review, *J. Hazard. Mater.* 274 (2014) 443–454.
- [15] Z. Du, S. Deng, Y. Chen, B. Wang, J. Huang, Y. Wang, G. Yu, Removal of perfluorinated carboxylates from washing wastewater of perfluorooctanesulfonyl fluoride using activated carbons and resins, *J. Hazard. Mater.* 286 (2015) 136–143.
- [16] Q. Yu, R. Zhang, S. Deng, J. Huang, G. Yu, Sorption of perfluorooctane sulfonate and perfluorooctanoate on activated carbons and resin: kinetic and isotherm study, *Water Res.* 43 (2009) 1150–1158.
- [17] S. Deng, Y. Nie, Z. Du, Q. Huang, P. Meng, B. Wang, J. Huang, G. Yu, Enhanced adsorption of perfluorooctane sulfonate and perfluorooctanoate by bamboo-derived granular activated carbon, *J. Hazard. Mater.* 282 (2015) 150–157.
- [18] Y. Wang, J. Niu, Y. Li, T. Zheng, Y. Xu, Y. Liu, Performance and mechanisms for removal of perfluorooctanoate (PFOA) from aqueous solution by activated carbon fiber, *RSC Adv.* 5 (2015) 86927–86933.
- [19] K. Liu, S. Zhang, X. Hu, K. Zhang, A. Roy, G. Yu, Understanding the adsorption of PFOA on MIL-101(Cr)-based anionic-exchange metal-organic frameworks: comparing DFT calculations with aqueous sorption experiments, *Environ. Sci. Technol.* 49 (2015) 8657–8665.
- [20] P. Punyapalukul, K. Suksomboon, P. Prarat, S. Khaodhiar, Effects of surface functional groups and porous structures on adsorption and recovery of perfluorinated compounds by inorganic porous silicas, *Sep. Sci. Technol.* 48 (2013) 775–788.
- [21] B. Bhattarai, M. Muruganandham, R.P. Suri, Development of high efficiency silica coated beta-cyclodextrin polymeric adsorbent for the removal of emerging contaminants of concern from water, *J. Hazard. Mater.* 273 (2014) 146–154.
- [22] X. Li, S. Chen, X. Quan, Y. Zhang, Enhanced adsorption of PFOA and PFOS on multiwalled carbon nanotubes under electrochemical assistance, *Environ. Sci. Technol.* 45 (2011) 8498–8505.

- [23] G. Ming, H. Duan, X. Meng, G. Sun, W. Sun, Y. Liu, L. Lucia, A novel fabrication of monodisperse melamine–formaldehyde resin microspheres to adsorb lead (II), *Chem. Eng. J.* 288 (2016) 745–757.
- [24] Y. Wu, Y. Li, L. Qin, F. Yang, D. Wu, Monodispersed or narrow-dispersed melamine–formaldehyde resin polymer colloidal spheres: preparation, size-control, modification, bioconjugation and particle formation mechanism, *J. Mater. Chem. B* 1 (2013) 204–212.
- [25] H. Zhou, S. Xu, H. Su, M. Wang, W. Qiao, L. Ling, D. Long, Facile preparation and ultra-microporous structure of melamine–resorcinol–formaldehyde polymeric microspheres, *Chem. Commun.* 49 (2013) 3763–3765.
- [26] H. Daiguji, T. Makuta, H. Kinoshita, T. Oyabu, F. Takemura, Fabrication of hollow melamine–formaldehyde microcapsules from microbubble templates, *J. Phys. Chem. B* 111 (2007) 8879–8884.
- [27] I.W. Cheong, J.S. Shin, J.H. Kim, S.J. Lee, Preparation of monodisperse melamine–formaldehyde microspheres via dispersed polycondensation, *Macromol. Res.* 12 (2004) 225–232.
- [28] Y. Wang, Y. Xie, Y. Zhang, S. Tang, C. Guo, J. Wu, R. Lau, Anionic and cationic dyes adsorption on porous poly-melamine–formaldehyde polymer, *Chem. Eng. Res. Des.* 114 (2016) 258–267.
- [29] Z. Lv, D. Zhao, S. Xu, Facile synthesis of mesoporous melamine–formaldehyde spheres for carbon dioxide capture, *RSC Adv.* 6 (2016) 59619–59623.
- [30] M.X. Tan, Y.N. Sum, J.Y. Ying, Y. Zhang, A mesoporous poly-melamine–formaldehyde polymer as a solid sorbent for toxic metal removal, *Energy Environ. Sci.* 6 (2013) 3254–3259.
- [31] S. Kawaguchi, A. Yekta, M.A. Winnik, Surface characterization and dissociation properties of carboxylic acid core–shell latex particle by potentiometric and conductometric titration, *J. Colloid Interface Sci.* 176 (1995) 362–369.
- [32] B. Tomita, Melamine–formaldehyde resins: molecular species distributions of methylolmelamines and some kinetics of methylolation, *J. Polym. Sci. Polym. Ed.* 15 (1977) 2347–2365.
- [33] M.L. Scheepers, P.J. Adriaenssens, J.M. Gelan, R.A. Carleer, D.J. Vanderzande, N.K. De Vries, P.M. Brandts, Demonstration of methylene–ether bridge formation in melamine–formaldehyde resins, *J. Polym. Sci. A–Polym. Chem.* 33 (1995) 915–920.
- [34] B. Tomita, H. Ono, Melamine–formaldehyde resins: constitutional characterization by fourier transform ^{13}C -NMR spectroscopy, *J. Polym. Sci. Polym. Ed.* 17 (1979) 3205–3215.
- [35] A. Aydın, M. İmamoglu, M. Gülfen, Separation and recovery of gold (III) from base metal ions using melamine–formaldehyde–thiourea chelating resin, *J. Appl. Polym. Sci.* 107 (2008) 1201–1206.
- [36] Z.E. Mohamed, H.M. Fahmy, M.H. Abo-Shosha, N.A. Ibrahim, Preparation, characterization, and utilization of melamine formaldehyde/polyaspartic acid/sawdust cation exchanger, *Polym. Plast. Technol.* 44 (2005) 97–110.
- [37] C.Y. Tang, Q. Shiang Fu, D. Gao, C.S. Criddle, J.O. Leckie, Effect of solution chemistry on the adsorption of perfluorooctane sulfonate onto mineral surfaces, *Water Res.* 44 (2010) 2654–2662.
- [38] F. Wang, K. Shih, Adsorption of perfluorooctanesulfonate (PFOS) and perfluorooctanoate (PFOA) on alumina: influence of solution pH and cations, *Water Res.* 45 (2011) 2925–2930.
- [39] Q. Yu, S. Deng, G. Yu, Selective removal of perfluorooctane sulfonate from aqueous solution using chitosan-based molecularly imprinted polymer adsorbents, *Water Res.* 42 (2008) 3089–3097.
- [40] K.-U. Goss, The pKa Values of PFOA and other highly fluorinated carboxylic acids, *Environ. Sci. Technol.* 42 (2008) 456–458.
- [41] A.H. Mollah, C.W. Robinson, Pentachlorophenol adsorption and desorption characteristics of granular activated carbon – I. Isotherms, *Water Res.* 30 (1996) 2901–2906.
- [42] S. Li, Q. Zhang, Geochemistry of the upper Han River basin, China, 1: spatial distribution of major ion compositions and their controlling factors, *Appl. Geochem.* 23 (2008) 3535–3544.
- [43] S. Taguchi, K. Takahashi, N. Hata, I. Kasahara, X-ray fluorescence spectrometric determination of sulfur-containing anionic surfactants in water after their enrichment on a membrane filter as an ion-pair complex with a cationic surfactant, *Analyst* 126 (2001) 2078–2081.
- [44] C. Zhong, M. He, H. Liao, B. Chen, C. Wang, B. Hu, Polydimethylsiloxane/covalent triazine frameworks coated stir bar sorptive extraction coupled with high performance liquid chromatography–ultraviolet detection for the determination of phenols in environmental water samples, *J. Chromatogr. A* 1441 (2016) 8–15.
- [45] E. Bianchi, G. Lessing, K.R. Brina, L. Angeli, N.B. Andriguetti, J.R. Peruzzo, C.A. do Nascimento, F.R. Spilki, A.L. Ziulkoski, L.B. da Silva, Monitoring the genotoxic and cytotoxic potential and the presence of pesticides and hydrocarbons in water of the Sinos River basin, Southern Brazil, *Arch. Environ. Contam. Toxicol.* (2017), <http://dx.doi.org/10.1007/s00244-016-0334-0>.
- [46] S.D. Kim, J. Cho, I.S. Kim, B.J. Vanderford, S.A. Snyder, Occurrence and removal of pharmaceuticals and endocrine disruptors in South Korean surface, drinking, and waste waters, *Water Res.* 41 (2007) 1013–1021.
- [47] X. Qin, F. Liu, G. Wang, G. Huang, Adsorption of humic acid from aqueous solution by hematite: effects of pH and ionic strength, *Environ. Earth. Sci.* 73 (2014) 4011–4017.
- [48] Y.S. Ho, G. McKay, Pseudo-second order model for sorption processes, *Process Biochem.* 34 (1999) 451–465.